Original Article | Neuroimaging and Head & Neck

eISSN 2005-8330
https://doi.org/10.3348/kjr.2023.0490
Korean J Radiol 2023;24(11):1131-1141

Korean Journal of Radiology
KJR

Cortical Iron Accumulation as an Imaging Marker for Neurodegeneration in Clinical Cognitive Impairment Spectrum: A Quantitative Susceptibility Mapping Study

Hyeong Woo Kim[1]*, Subin Lee[2]*, Jin Ho Yang[1], Yeonsil Moon[3,4], Jongho Lee[2], Won-Jin Moon[1,4]

[1]Department of Radiology, Konkuk University Medical Center, Seoul, Republic of Korea
[2]Laboratory for Imaging Science and Technology, Department of Electrical and Computer Engineering, Seoul National University, Seoul, Republic of Korea
[3]Department of Neurology, Konkuk University Medical Center, Seoul, Republic of Korea
[4]Research Institute of Medical Science, Konkuk University School of Medicine, Seoul, Republic of Korea

Objective: Cortical iron deposition has recently been shown to occur in Alzheimer's disease (AD). In this study, we aimed to evaluate how cortical gray matter iron, measured using quantitative susceptibility mapping (QSM), differs in the clinical cognitive impairment spectrum.

Materials and Methods: This retrospective study evaluated 73 participants (mean age ± standard deviation, 66.7 ± 7.6 years; 52 females and 21 males) with normal cognition (NC), 158 patients with mild cognitive impairment (MCI), and 48 patients with AD dementia. The participants underwent brain magnetic resonance imaging using a three-dimensional multi-dynamic multi-echo sequence on a 3-T scanner. We employed a deep neural network (QSMnet+) and used automatic segmentation software based on FreeSurfer v6.0 to extract anatomical labels and volumes of interest in the cortex. We used analysis of covariance to investigate the differences in susceptibility among the clinical diagnostic groups in each brain region. Multivariable linear regression analysis was performed to study the association between susceptibility values and cognitive scores including the Mini-Mental State Examination (MMSE).

Results: Among the three groups, the frontal ($P < 0.001$), temporal ($P = 0.004$), parietal ($P = 0.001$), occipital ($P < 0.001$), and cingulate cortices ($P < 0.001$) showed a higher mean susceptibility in patients with MCI and AD than in NC subjects. In the combined MCI and AD group, the mean susceptibility in the cingulate cortex ($\beta = -216.21$, $P = 0.019$) and insular cortex ($\beta = -276.65$, $P = 0.001$) were significant independent predictors of MMSE scores after correcting for age, sex, education, regional volume, and APOE4 carrier status.

Conclusion: Iron deposition in the cortex, as measured by QSMnet+, was higher in patients with AD and MCI than in NC participants. Iron deposition in the cingulate and insular cortices may be an early imaging marker of cognitive impairment related neurodegeneration.

Keywords: Iron; Quantitative evaluation; Cognition disorders; Magnetic resonance imaging

INTRODUCTION

Accumulating evidence suggests an important role of brain iron in various neurodegenerative disorders such as Parkinson's disease and Alzheimer's disease (AD). Iron is an essential component of brain development, neurotransmitter metabolism, myelin synthesis, oxidative phosphorylation, and DNA synthesis [1]. With aging, iron gradually accumulates in the brain, particularly in the deep gray matter and cerebral cortex [2,3]. However, the

Received: March 10, 2023 **Revised:** July 19, 2023 **Accepted:** August 22, 2023
*These authors contributed equally to this work.
Corresponding author: Won-Jin Moon, MD, PhD, Department of Radiology, Konkuk University Medical Center, Konkuk University School of Medicine, 120-1 Neungdong-ro, Gwangjin-gu, Seoul 05030, Republic of Korea
• E-mail: mdmoonwj@kuh.ac.kr

underlying causes of iron accumulation remain unclear. Excessive iron can induce oxidative damage by increasing toxic oxygen radical species [1], and may exacerbate disease pathology, such as amyloid and tau pathology, and augment neuroinflammation accordingly [4,5].

Elevated brain iron levels have been studied in aging and in many neurodegenerative diseases using magnetic resonance (MR) with T2* contrast [3,6-8]. Iron accumulation in deep gray matter has been extensively investigated in various neurodegenerative disorders, including AD [7-9]. Recently, cortical iron has been increasingly studied using both postmortem and in vivo imaging in normal elderly individuals [3], individuals on the cognitive impairment spectrum [8], and individuals with AD [10-12]. However, few studies have reported on the relationship between cortical iron deposition and general cognition [13,14]. Moreover, the independent role of iron accumulation in brain atrophy has not yet been clearly elucidated in the context of the cognitive impairment spectrum.

Quantitative susceptibility mapping (QSM) is a widely accepted method for measuring tissue iron. However, cortical iron measurement using QSM remains challenging because of the loss of detailed cortical ribbon structure during processing [15]. Recently developed deep neural network-based methods, referred to as QSMnet, have been applied to patient data and have successfully delineated cortical regions [15]. A subsequent study introduced a method to further improve the linearity of the susceptibility estimation in QSMnet. The refined deep neural network, QSMnet+, enables the quantification of a wide range of susceptibility values [16].

In this study, we hypothesized that the susceptibility of the cortex differs according to the stage of the clinical cognitive impairment spectrum and that the susceptibility of the cortex is correlated with the general cognition score. Therefore, we aimed to evaluate how cortical gray matter iron, measured using QSMnet+, differs and how susceptibilities are related to general cognition in the clinical cognitive impairment spectrum.

MATERIALS AND METHODS

Study Design and Patient Selection

This retrospective study was approved by Konkuk University Medical Center institutional review board (No.2020-09-030), and the requirement for informed consent was waived because of the retrospective nature of the study.

Participants with mild cognitive impairment (MCI) (n = 158), probable AD dementia (n = 48), and normal cognition

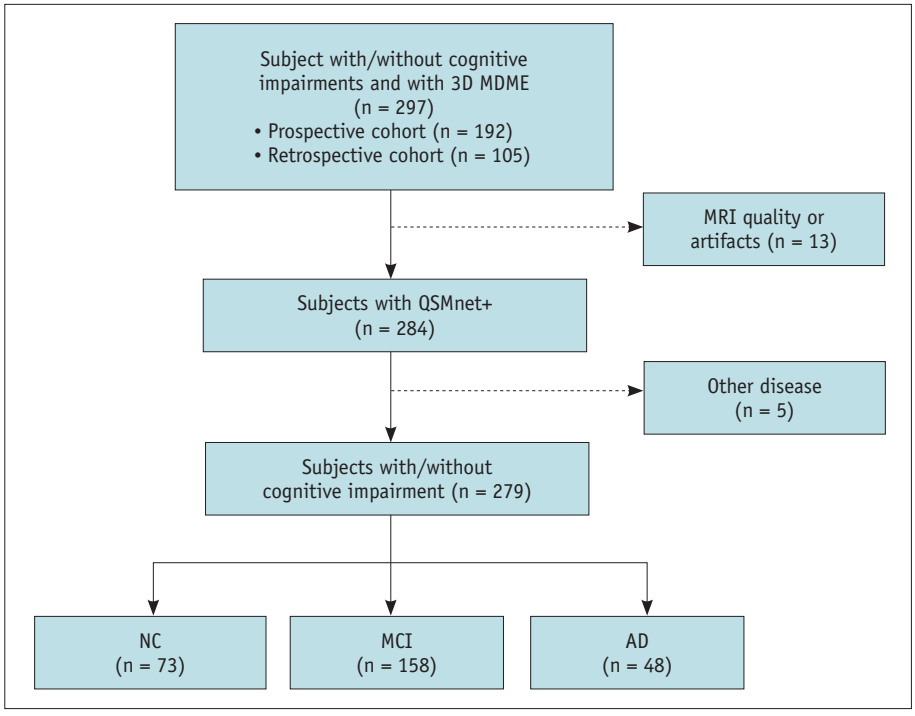

Fig. 1. Flowchart of the study data acquisition. 3D MDME = three-dimensional multidynamic multi-echo, MRI = magnetic resonance imaging, NC = normal cognition, MCI = mild cognitive impairment, AD = Alzheimer's dementia

https://doi.org/10.3348/kjr.2023.0490

Korean Journal of Radiology
KJR

(NC) (n = 73) were included in this retrospective study. Participants with NC, MCI, or AD were recruited from a retrospective registry and a prospective cohort of consecutive patients who visited the Memory Clinic of the Konkuk University Medical Center and underwent magnetic resonance imaging (MRI) examination between January 2013 and May 2020 (Fig. 1). Among the 192 participants in the prospective cohort, QSMnet+ data of 142 participants had been previously studied for relationship between cortical iron and diabetes mellitus [17]. The inclusion criteria for patients with MCI and AD were: 1) diagnosis of MCI or AD according to established criteria and 2) raw MR data for QSM generation. The exclusion criteria were: 1) severe MR artifacts and 2) presence or history of other neurological diseases, such as Parkinson's disease, multiple sclerosis or encephalitis, malignancy, stroke, or brain surgery). The diagnoses of MCI and probable AD dementia were based on the Petersen et al. [18] criteria and recommendations from the National Institute on Aging Alzheimer's Association workgroups on diagnostic guidelines for MCI and AD [19,20]. Thus, 48 participants with AD dementia were diagnosed with an intermediate-to-high probability of AD etiology based on biomarker criteria [19].

The 73 participants with NC were recruited from the relatives of patients who visited the memory clinic, volunteers who applied for comprehensive dementia evaluation, and participants who had subjective cognitive complaints. These individuals visited the memory clinic and underwent MR examination using the same protocol as the patients. All participants met the following criteria: absence of a history of medical disease affecting cognitive function [21], absence of a history of other neurologic diseases as described above, no objective cognitive impairment, and no evidence of structural lesions such as tumors, infarctions, or severe artifacts on brain MRI. The cognition of NC participants was above 1.0 standard deviation compared to appropriate normative data for the abbreviated version or comprehensive version of neuropsychiatric tests.

Patient demographics, education level, APOE4 genotyping, global cognition scores (clinical dementia rating [CDR] score, Mini-Mental State Examination [MMSE] score, and Clinical Dementia Rating Sum of Boxes [CDRSB] score), and brain MRI scans were assessed. We analyzed laboratory test results to differentiate clinical cognitive diseases from other medical conditions that mimic dementia symptoms. The vascular risk burden was determined as the sum of the following factors: diabetes, hypertension, dyslipidemia, history of smoking or current smoking, cardiovascular disease history, and minor stroke history [9,22].

Structural MRI was performed to exclude focal masses, large-vessel infarctions, and inflammatory lesions. Additionally, imaging factors for microvascular pathology were assessed (white matter hyperintensity visual scales, lacunae, and microbleeds) [22]. For microbleed assessment, the number of microbleeds was defined as a T2* hypointensity with a size of 2–10 mm on susceptibility-weighted imaging and QSM images [23]. The microbleed number was used as an imaging covariate in the subsequent statistical analysis.

MRI Acquisition

All patients underwent MRI using the same 3-T unit (MAGNETOM Skyra; Siemens Healthineers) with a 20-channel coil and the following MRI sequences: sagittal 3D T1-weighted magnetization-prepared rapid acquisition of gradient echo (repetition time/echo time/inversion time [ms] = 2300/2.98/900, sagittal 3D or axial 2D fluid-attenuated inversion recovery (5000/393/1800 or 9000/95/2500) and axial 3D multi-dynamic multi-echo (81/8.9, 6 echoes with echo-spacing of 4.9 ms) (Supplementary Table 1). This 3D multi-dynamic multi-echo sequence was used for QSM reconstruction from the raw imaging data.

Brain Volumetry

The segmented intracranial regional volume was determined using FreeSurfer 6.0 (http://surfer.nmr.mgh.harvard.edu/), which performs automated image analysis of brain structures using 3D T1-weighted magnetization-prepared rapid gradient echo images. The segmentation results were checked by a researcher with 10 years of experience in neuroimaging. The cortical parcellation results were combined into lobar regions to obtain the region of interest (ROI) masks of the frontal, parietal, occipital, temporal, insular, and cingulate cortices [24]. The volumes of the six lobar regions were obtained. To compensate for individual variations in head size [25], each regional volume was normalized to the total intracranial volume (ICV). The resulting ICV-adjusted ROI volumes were used for the subsequent statistical analyses.

QSM Analysis

For QSM reconstruction, we used a neural-network-based method called QSMnet+ [16]. Compared to the original QSMnet [15], which was trained on healthy participants,

 https://doi.org/10.3348/kjr.2023.0490

QSMnet+ was trained on a wider range of susceptibility values to improve generalizability to cases where higher susceptibility values were found, such as in patients with hemorrhage. QSMnet+ was assessed on computer-simulated lesions (ranging from -1.4 ppm to +1.4 ppm) and hemorrhagic patients and was validated to have fewer artifacts compared to those of conventional QSM maps [16]. QSMnet+ requires the input to have an isotropic voxel size of 1 x 1 x 1 mm because it has been trained to read isotropic 1 x 1 x 1 mm images. To match the required resolution, the 0.6 x 0.6 x 2 mm gradient echo images were first resampled to 1 x 1 x 1 mm in k-space, then inverse-Fourier transformed. From these image data, the magnitude image was used to generate a brain mask using Brain Extraction Tool (BET; FSL) [26]. Within the brain mask, the phase image was unwrapped using Laplacian phase unwrapping [27]. The background field was removed using V-SHARP [28]. The local field map was then input into QSMnet+ to obtain the final QSM map (Fig. 2). The QSM map and coregistration results were checked by a researcher with 10 years of neuroimaging experience and a neuroradiologist with 22 years of experience.

Statistical Analysis

After checking for normality using the Kolmogorov-Smirnov test, analysis of variance (ANOVA) was used for continuous variables, and the chi-square test was used for categorical variables to compare baseline characteristics between patient groups. To compare the susceptibilities of the cortical regions between the groups, we used ANCOVA with adjustments for age, sex, number of microbleeds, and each region's respective ICV-adjusted volumes. Post-hoc tests were performed using the Bonferroni correction for multiple comparisons. Pearson's correlation analysis was performed to assess the simple univariable relationship between susceptibility values in cortical regions and cognitive scores (MMSE and CDRSB). Finally, the relationship between the susceptibility of each cortical gray matter and the cognitive score in the study group was evaluated using multiple linear regression after adjusting for age, sex, education, APOE4 carrier status, microbleed number, and ICV-adjusted ROI volumes as covariates. All statistical analyses were performed using IBM SPSS Statistics for Windows (version 26.0; IBM Corp.). *P*-values of less than 0.05 were considered statistically significant.

RESULTS

Clinical Characteristics of Participants

A summary of the participant characteristics is presented in Table 1. A total of 279 participants (82 males and 197

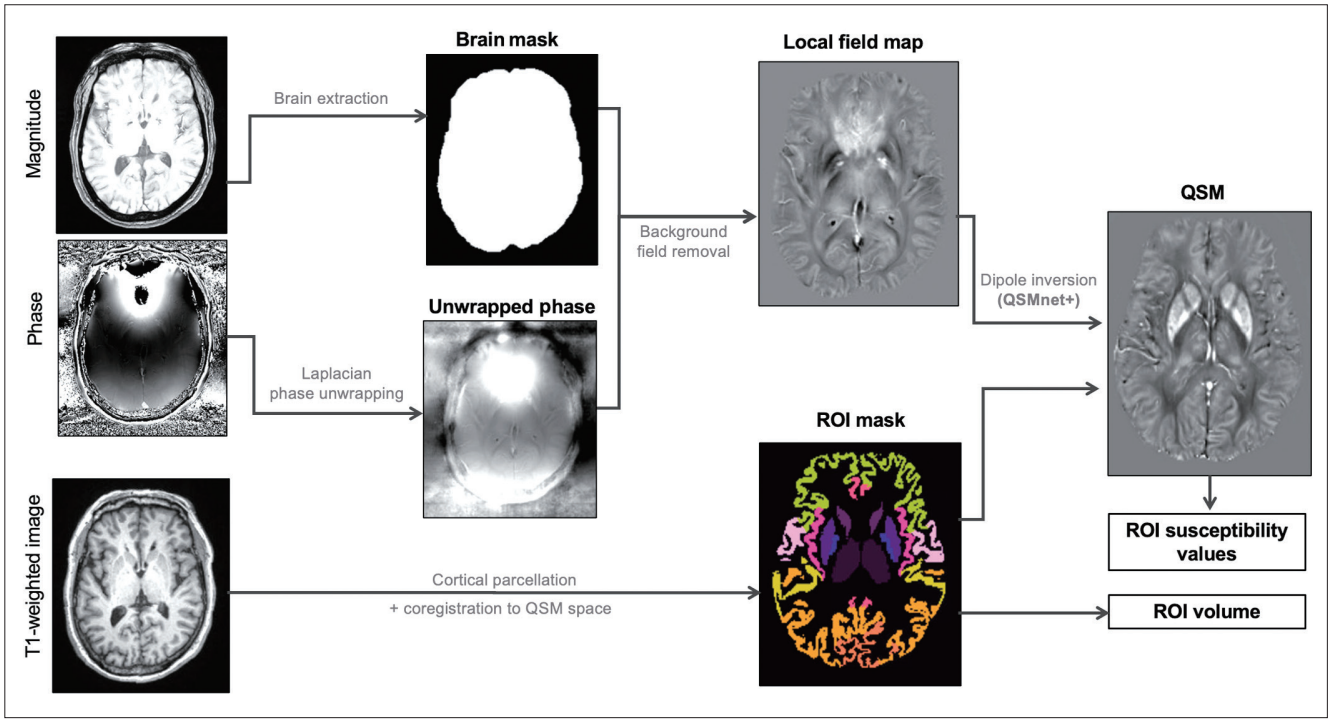

Fig. 2. Pipeline overview of QSMnet+. QSM = Quantitative susceptibility mapping, ROI = region of interest

https://doi.org/10.3348/kjr.2023.0490

Korean Journal of Radiology
KJR

females) were included in this study. The mean age of the participants was 66.7 ± 7.6 (standard deviation) years, 70.3 ± 7.2 years, and 74.3 ± 7.2 years in the NC, MCI, and AD dementia groups, respectively. The number of years of education decreased as the severity of the diagnosis increased (P < 0.001). APOE4 positive ratio were 18.2%, 33.6%, and 43.8% in the NC, MCI, and AD dementia groups, respectively (P = 0.031). The CDR and CDRSB scores were higher, and the MMSE scores were lower, in the more severe disease group. Vascular risk burden showed no significant relationship among the three groups.

Table 1. Clinicodemographic features of the study population

Characteristic	NC (n = 73)	MCI (n = 158)	AD (n = 48)	*P*
Age, yr	66.7 ± 7.6	70.3 ± 7.2	74.3 ± 7.2	< 0.001
Sex, female	52 (71.2)	111 (70.3)	34 (70.8)	0.988
Education, yr	11.9 ± 4.6	9.2 ± 4.9	6.6 ± 5.0	< 0.001
APOE4 positive	8 (18.2)	49 (33.6)	21 (43.8)	0.031
CDR				< 0.001
0	37 (50.7)	18 (11.5)	0 (0.0)	
0.5	36 (49.3)	136 (87.2)	18 (37.5)	
1	0 (0.0)	2 (1.3)	30 (62.5)	
MMSE	27.9 ± 1.8	25.2 ± 3.5	17.8 ± 5.2	< 0.001
CDRSB	0.5 ± 0.6	1.5 ± 1.0	5.4 ± 2.9	< 0.001
Vascular risk burden	1.2 ± 1.3	1.4 ± 1.3	1.1 ± 1.0	0.189
Microbleed, number of lesions	0.5 ± 1.6	0.9 ± 2.9	3.8 ± 12.1	0.089

Data are presented as the n (%) or mean ± standard deviation. NC = normal cognition, MCI = mild cognitive impairment, AD = Alzheimer's disease, CDR = clinical dementia rating, MMSE = Mini-mental State Examination, CDRSB = Clinical Dementia Rating Sum of Boxes, APOE4 = apolipoprotein E4

Comparison of Susceptibility in Each Cortical Gray Matter Region by Clinical Diagnosis Group

After adjusting for age, sex, and adjusted volume of each region, post-hoc comparisons revealed that the susceptibility of the whole cortex was higher in AD dementia (-0.002 ± 0.003 ppm) and MCI (-0.003 ± 0.003 ppm) than in NC (-0.005 ± 0.003 ppm) (F = 8.277, P < 0.001) (Fig. 3). However, post-hoc comparisons revealed no significant differences in susceptibility between the MCI and AD dementia groups. Compared with the NC group, the AD dementia and MCI groups showed significantly higher susceptibility in the frontal, temporal, parietal, occipital, and cingulate cortices. However, no significant group differences were observed for the insular cortex (Table 2).

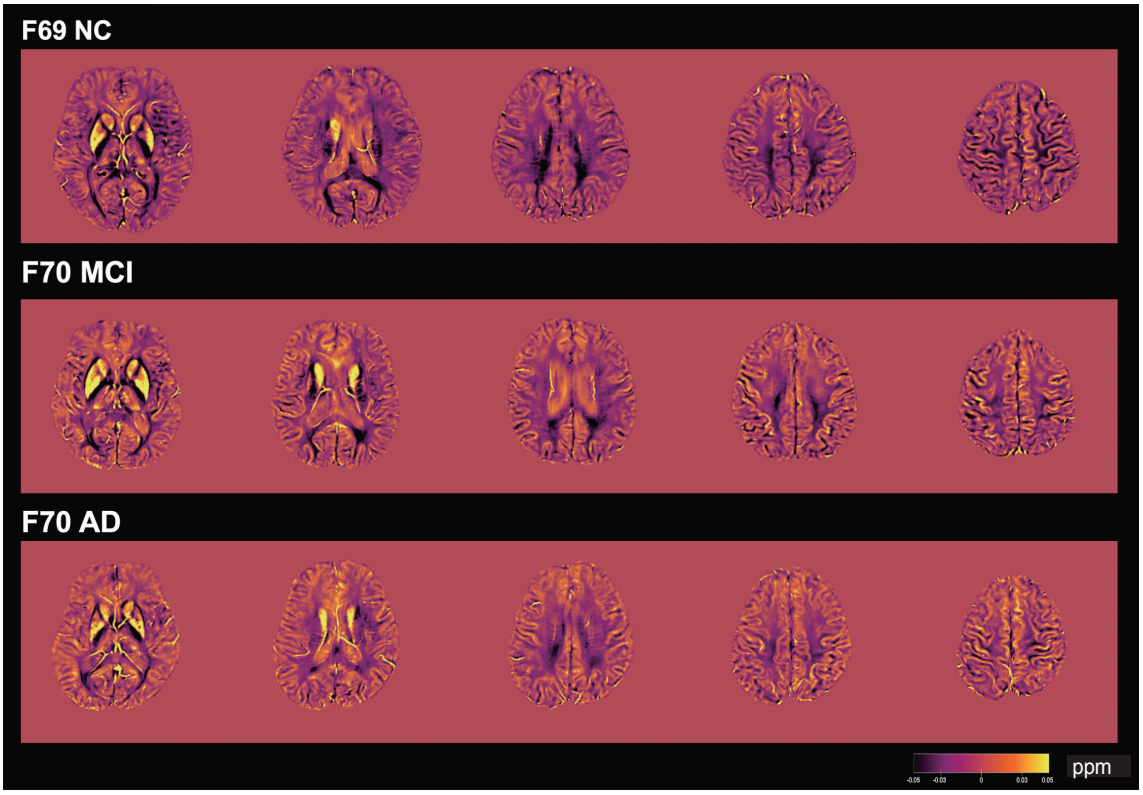

Fig. 3. Exemplary cases. Note the higher susceptibility in patients with MCI and AD compared to the cognitively normal participants. NC = normal cognition, MCI = mild cognitive impairment, AD = Alzheimer's dementia

https://doi.org/10.3348/kjr.2023.0490

Table 2. Comparison of susceptibility in each cortical gray matter region by clinical diagnosis group

Brain region	Susceptibility (ppm)*			ANCOVA†		
	NC	MCI	AD	F	*P*	Post-hoc
Whole cortex	-0.0046 ± 0.0029	-0.00265 ± 0.0035	-0.0016 ± 0.0030	8.389	< 0.001	NC vs. MCI (*P* < 0.001), NC vs. AD (*P* = 0.003)
Frontal cortex	-0.0034 ± 0.0029	-0.0016 ± 0.0033	-0.0007 ± 0.0030	8.200	< 0.001	NC vs. MCI (*P* < 0.001), NC vs. AD (*P* = 0.004)
Temporal cortex	-0.0055 ± 0.0030	-0.0036 ± 0.0036	-0.0028 ± 0.0031	5.770	0.004	NC vs. MCI (*P* = 0.003), NC vs. AD (*P* = 0.051)
Parietal cortex	-0.0044 ± 0.0030	-0.0024 ± 0.0037	-0.0012 ± 0.0032	6.735	0.001	NC vs. MCI (*P* = 0.002), NC vs. AD (*P* = 0.013)
Occipital cortex	-0.0046 ± 0.0031	-0.0025 ± 0.0038	-0.0014 ± 0.0033	7.852	< 0.001	NC vs. MCI (*P* < 0.001), NC vs. AD (*P* = 0.004)
Cingulate cortex	-0.0053 ± 0.0036	-0.0031 ± 0.0040	-0.0016 ± 0.0033	8.065	< 0.001	NC vs. MCI (*P* = 0.002), NC vs. AD (*P* = 0.001)
Insular cortex	-0.0127 ± 0.0041	-0.0121 ± 0.0040	-0.0104 ± 0.0040	2.024	0.134	NA

*Data are mean ± standard deviation, †Results of ANCOVA controlled for age, sex, microbleed number and each region's respective ICV-adjusted volume. Multiple comparisons corrected using the Bonferroni method (degrees of freedom: 2, 279).
ANCOVA = analysis of covariance, NC = normal cognition, MCI = mild cognitive impairment, AD = Alzheimer's disease, NA = not applicable, ICV = intracranial volume

Relationship between Susceptibility in Each Brain Region and Global Cognitive Scores: Univariable Analysis

There was a negative correlation between MMSE scores and susceptibility in the cingulate (r = -0.18, P = 0.01) and insular (r = -0.225, P = 0.001) cortices The CDRSB score showed a positive correlation with the whole (r = 0.162, P = 0.021), parietal (r = 0.177, P = 0.012), occipital (r = 0.146, P = 0.038), cingulate (r = 0.194, P = 0.006), and insular (r = 0.223, P = 0.001) cortices (Table 3).

Relationship between Susceptibility in Each Brain Region and Global Cognitive Scores: Multivariable Analysis

In the combined MCI and AD dementia group, higher cortical susceptibility in the cingulate (β = -181.464, P = 0.048) and insular (β = -260.246, P = 0.002) cortices were the only two valuable susceptibility markers for predicting lower MMSE scores (Table 4). After adjusting for covariates, higher susceptibility of the insular cortex was associated with higher CDRSB scores (β = 102.04, P = 0.023). No significant association was found between the cognitive scores and susceptibility to other cortical regions.

When the whole group was considered, both the susceptibilities of the cingulate and insular cortices were valuable susceptibility markers for predicting MMSE decline (β = -149.599, P = 0.048; β = -221.946, P = 0.002) and worsened CDRSB scores (β = 84.344, P = 0.034; β = 93.542, P = 0.014) (Table 5).

Table 3. Simple univariable correlations between global cognitive scores and susceptibility in each brain region (in the MCI and AD population)

	MMSE		CDRSB	
	r	*P*	*r*	*P*
Cortical gray matter				
Whole cortex	-0.132	0.059	0.162	0.021
Frontal cortex	-0.117	0.095	0.138	0.050
Temporal cortex	-0.108	0.122	0.134	0.057
Parietal cortex	-0.129	0.065	0.177	0.012
Occipital cortex	-0.111	0.115	0.146	0.038
Cingulate cortex	-0.180	0.010	0.194	0.006
Insular cortex	-0.225	0.001	0.223	0.001

MCI = mild cognitive impairment, AD = Alzheimer's disease, MMSE = Mini-Mental State Examination, CDRSB = Clinical Dementia Rating Sum of Boxes

DISCUSSION

Using deep neural network-based QSMnet +, we found that the susceptibility of the whole cortex was higher in patients with cognitive impairment than in controls. Post-hoc analysis showed no difference in cortical susceptibility between the MCI and AD dementia groups. In the combined MCI and AD dementia group, higher susceptibility in the cingulate and insular cortices was associated with worse MMSE and CDRSB scores, respectively, even after controlling for age, sex, educational level, regional brain volume, and APOE4 status.

https://doi.org/10.3348/kjr.2023.0490

Korean Journal of Radiology
KJR

Table 4. Multivariable analysis of the relationship between cognitive scores and brain iron levels in cognitively impaired patients (MCI + AD population)

	MMSE		CDRSB	
	β (SE)	*P*	β (SE)	*P*
Cortical gray matter				
Whole cortex	-90.154 (98.683)	0.362	42.691 (53.143)	0.423
Frontal cortex	-112.499 (107.082)	0.295	46.429 (57.660)	0.422
Temporal cortex	-84.031 (95.754)	0.381	30.662 (50.556)	0.545
Parietal cortex	-81.378 (94.438)	0.390	46.829 (50.757)	0.357
Occipital cortex	-96.874 (97.929)	0.324	52.889 (52.654)	0.316
Cingulate cortex	-181.464 (91.290)	0.048	71.749 (49.125)	0.146
Insular cortex	-260.246 (82.293)	0.002	94.468 (44.324)	0.034

Model adjusted for age, sex, education, APOE4 carrier status, and ICV-adjusted ROI volume.
MCI = mild cognitive impairment, AD = Alzheimer's disease, MMSE = Mini-Mental State Examination, CDRSB = Clinical Dementia Rating Sum of Boxes, SE = standard error, ICV = intracranial volume, ROI = region of interest, APOE4 = apolipoprotein E4

Table 5. Multivariable analysis of the relationship between cognitive scores and brain iron levels across the cognitive spectrum (the entire participants)

	MMSE		CDRSB	
	β (SE)	*P*	β (SE)	*P*
Cortical gray matter				
Whole cortex	-84.567 (83.878)	0.314	65.465 (44.114)	0.139
Frontal cortex	-94.290 (90.238)	0.297	67.703 (47.680)	0.157
Temporal cortex	-77.537 (81.889)	0.345	52.161 (42.658)	0.223
Parietal cortex	-65.508 (79.885)	0.413	58.569 (41.884)	0.163
Occipital cortex	-91.735 (81.509)	0.262	69.444 (43.075)	0.108
Cingulate cortex	-149.599 (75.229)	0.048	84.344 (39.590)	0.034
Insular cortex	-221.946 (71.335)	0.002	93.542 (37.637)	0.014

Model adjusted for age, sex, education, APOE4 carrier status, and ICV-adjusted ROI volume.
MMSE = Mini-Mental State Examination, CDRSB = Clinical Dementia Rating Sum of Boxes, SE = standard error, ICV = intracranial volume, ROI = region of interest, APOE4 = apolipoprotein E4

Our results are consistent with those of previous studies showing that cortical iron is elevated in AD in postmortem studies [10,14], QSM studies [29], T2* imaging at 7T [30], and R2* relaxation imaging [12]. Non-heme iron accumulation has been observed in the frontal cortex of patients with AD in conjunction with amyloid plaques and activated microglia but not in neurofibrillary tangles and neuropil threads [10]. Additionally, cortical iron was significantly correlated with Braak stage, amyloid plaque score, and degree of local tau pathology [10]. Interestingly, iron was also found in myelinated fibers of the middle cortical layers [10]. Contrastingly, Ayton et al. [14] reported that iron accumulation was only correlated with tau pathology but not with amyloid plaques. In their study, elevated iron levels in the inferior temporal cortex were observed in the postmortem brains of patients diagnosed with clinical dementia and AD pathology [14]. This implies that cortical iron levels can be used to distinguish between clinical dementia and non-dementia groups in patients with high AD pathology [14].

In an imaging study, Kim et al. [29] reported a voxel-wise comparison of QSM in a small sample, where they found a significant difference between 19 NC and 19 MCI cases for the precuneus and cingulate cortices, 19 MCI and 19 AD cases for the neocortex, and 19 NC and 19 AD cases for the precuneus, cingulate cortex, and neocortex [29]. A later study by Damulina et al. [12] using R2* to measure brain iron reported that brain iron was elevated in the total cortex of 100 patients with AD compared to 100 healthy controls ($P < 0.001$). However, they found an R2*difference only in the temporal and occipital lobes, but not in other cortical regions [12].

Conversely, our findings suggest that iron accumulation is more widespread across the entire cortex than reported in other 3T studies. Rather, our findings are consistent with a previous 7T study that showed an increasing cortical phase

 https://doi.org/10.3348/kjr.2023.0490

shift in the temporoparietal, frontal, and parietal regions [30]. Additionally, since we adjusted the regional cortical volume for susceptibility comparison among the groups, the finding that widespread iron differences were maintained, even when comparing NC and MCI, implies that cortical iron accumulation might be an early imaging marker that can distinguish NC from MCI.

In our study, the correlation between QSM values and cognitive decline, after controlling for regional volume, implied that cortical susceptibility (iron) is an imaging correlate of cognitive decline. In a study by Ayton et al., [14] amyloid positron emission tomography (PET) (+) groups showed higher susceptibility of the hippocampus, frontal lobe, and temporal lobe, correlating to lower cognitive performance in all five cognitive domains. Meanwhile, the amyloid PET (–) group showed only subtle decreases in language performance as susceptibility of the frontal and caudate nucleus increased and only modestly increased episodic memory as susceptibility of the hippocampus increased [13]. In a post-mortem study (n = 209) by Ayton et al. [14], higher cortical iron levels in the inferior temporal gyrus were associated with rapid cognitive decline, expressed as a composite of global cognition. Our findings corroborate previous findings regarding the close relationship between the susceptibility of the cortex and cognition scores.

Our findings underscore the role of the cingulate and insular cortices in general cognition. Pathologically, amyloid plaques accumulate in the cingulate cortex (along with the entorhinal cortex and hippocampus) in Thal phase 2 of AD-related amyloid-beta pathology, whereas amyloid plaques are first observed in the neocortex in Thal phase 1 [31]. A study found that the earliest uptake sites for amyloid PET include the posterior cingulate cortex, anterior cingulate cortex, isthmus of the cingulate cortex, and precuneus [32]. In another amyloid PET study, an uptake abnormality was most frequently observed in the cingulate cortex, followed by the orbitofrontal cortex, precuneus, insular cortex, and the associative, frontal, and occipital cortices [33]. Contrastingly, regarding neurofibrillary tangle (tau) pathology, both the cingulate and insular cortices are affected in stage IV AD [34].

Functionally, the posterior cingulate cortex is an important component of the default mode network, while the anterior cingulate and insular cortices are components of the salience network. These networks are interconnected and serve to maintain mental function in daily life. Thus, patients with AD show decreased resting-state activity in the posterior cingulate cortex [35], and decreased functional connectivity in the frontal insular and dorsal anterior cingulate cortices [36].

In this study, although insular cortex susceptibility did not differ among groups, we found a negative correlation between susceptibility and general cognition scores (CDRSB). This discrepancy may be attributed to the fact that general cognition scores are not the sole determinants of AD diagnosis and may reflect only a certain part of cognitive function or cognitive ability. Additionally, a binary disease diagnosis does not precisely capture the continuous spectrum of cognitive impairment, which may be better represented using cognitive scores. Our observation is in line with the observation that insular cortex atrophy is associated with the neuropsychiatric symptoms in AD [37,38]. Neuropsychiatric symptoms in AD are key factors in predicting functional status [39]. Impaired interoception owing to insular dysfunction leads to decreased decision-making abilities in dementia patients [40]. Besides AD-specific pathology, non-amyloid and non-tau pathologies, such as reactive astrogliosis, can also explain changes in insular cortex susceptibility [41,42].

QSM-based susceptibility may be affected by many potential constituents such as iron, myelin, amyloid, tau, and astrogliosis. Ayton et al. [13] suggested that iron accumulation might act synergistically with amyloid accumulation to exacerbate cognitive performance. Another study in healthy older adults found a statistically significant correlation between local susceptibility and ^{18}F-Flutametamol uptake, indicating local colocalization of iron with beta-amyloid deposition [43]. However, in patients with amyloid pathology (n = 237), tau PET uptake positively correlated with QSM susceptibility in the inferior temporal gyrus, where tau pathology is prominently affected in AD. Furthermore, one study has revealed that QSM susceptibility has a modulatory effect on the relationship between tau pathology and brain atrophy [11]. In a 7T postmortem study, T2* susceptibility-based contrast was mainly determined by iron content and myelin disorganization, and not by amyloid or tau [44]. Abundant iron is found in microglia, myelinated fibers, and amyloid plaques [44]. In another postmortem study, amyloid plaques were diamagnetic [45]. Subsequently, a postmortem study confirmed that iron was not related to amyloid plaque pathology, but was weakly related to tau pathology [14].

Therefore, we speculated that QSM-based susceptibility might be indicative of the role of neuroinflammation (not

https://doi.org/10.3348/kjr.2023.0490

Korean Journal of Radiology
KJR

amyloid/tau) in AD pathogenesis and might serve as an imaging marker of neuroinflammation, with pathological evidence of microglial activation and subsequent iron accumulation [46]. Specifically, QSM-based susceptibility might serve as an imaging marker related to amyloid imaging for abnormalities following amyloid beta immunotherapy [47]. One caveat of QSM might be that the co-localization of iron and amyloid plaques can alleviate the contrast effect of susceptibility, which could reduce the sensitivity of QSM in predicting cognitive decline. However, our findings suggest that QSM can be an effective imaging marker for predicting cognitive decline in the clinical AD spectrum, regardless of whether the amyloid pathology is positive or negative. An additional caveat is that QSM values may be influenced by vascular risk factors such as diabetes [21,17]. However, this cumulative impact of the vascular risk burden on QSM seems unlikely, considering that there was no significant difference in vascular risk burden among the groups in this study. We did not evaluate the effects of the individual vascular risk factors. Further studies with larger sample sizes and detailed analyses of individual vascular risk factors are necessary.

Our study had a few limitations. First, it was cross-sectional, and actual longitudinal changes could not be measured. Second, the clinical spectrum of patients with AD was considered the study cohort. Thus, our cohort might have included a mixed population of amyloid-positive and -negative participants. This may hinder further exploration of the relationship between iron levels and other pathological markers of AD. Third, the age difference between the groups may have contributed to iron measurement. To address this limitation, we used a relatively large consecutive sample (n = 279) and treated age as a covariate. Last, the low spatial resolution of the original image in the axial direction (0.6 x 0.6 x 2 mm) and the process of resampling to isotropic resolution (1 x 1 x 1 mm) may have resulted in some partial volume effects and affected accuracy of the cortical susceptibility measurements. In future studies, images acquired at an isotropic 1-mm resolution would be desirable. Nevertheless, our findings may represent the future role of QSM in predicting clinical cognitive decline, irrespective of the patient's AD pathological status.

In conclusion, higher QSM susceptibility in the cortex was associated with lower cognitive performance across the spectrum of clinical cognitive impairment in our study cohort. Our study suggests that iron deposition in the cingulate and insular cortices may be an early imaging marker of neurodegeneration related to cognitive impairment.

Supplement

The Supplement is available with this article at https://doi.org/10.3348/kjr.2023.0490.

Availability of Data and Material

The datasets generated or analyzed during the study are available from the corresponding author on reasonable request.

Conflicts of Interest

The authors have no potential conflicts of interest to disclose.

Author Contributions

Conceptualization: Won-Jin Moon. Data curation: Subin Lee, Yeonsil Moon. Formal analysis: Hyeong Woo Kim, Subin Lee, Jin Ho Yang, Jongho Lee, Won-Jin Moon. Funding acquisition: Won-Jin Moon. Investigation: Hyeong Woo Kim, Won-Jin Moon. Methodology: Subin Lee, Jongho Lee. Project administration: Won-Jin Moon. Resources: Jongho Lee. Software: Subin Lee. Supervision: Won-Jin Moon. Validation: Hyeong Woo Kim, Yeonsil Moon, Subin Lee, Won-Jin Moon. Visualization: Subin Lee. Writing—original draft: Hyeong Woo Kim, Subin Lee, Won-Jin Moon. Writing—review & editing: Subin Lee, Jin Ho Yang, Yeonsil Moon, Jongho Lee, Won-Jin Moon.

ORCID IDs

Hyeong Woo Kim
https://orcid.org/0000-0002-0253-3711
Subin Lee
https://orcid.org/0000-0001-7583-6468
Jin Ho Yang
https://orcid.org/0000-0003-4444-8993
Yeonsil Moon
https://orcid.org/0000-0001-7770-4127
Jongho Lee
https://orcid.org/0000-0002-9485-5434
Won-Jin Moon
https://orcid.org/0000-0002-8925-7376

Funding Statement

This work was supported by the National Research

Foundation of Korea (NRF) grant, funded by the Korean government (MSIP) (grant number 2020R1A2C1102896) and the Korea Health Technology R&D Project through the Korea Health Technology R&D Project through the Korea Health Industry Development Institute (KHIDI), funded by the Ministry of Health & Welfare, Republic of Korea (grant number HU21C0222).

Acknowledgments

The authors thank Hee Jin Kim, MD, PhD, from Hanyang University, Chung-Hwan Kang, RT, Ha-young Kim, BS, Su-ji Kim, RN, from Konkuk University Medical Center for their support in the patient recruitment, imaging data acquisition and management of this study.

Permission Statement

An unauthorized version of the Korean Mini-Mental State Examination (MMSE) was used by the study team without permission but this has been rectified with Psychological Assessment Resources Inc. The MMSE is a copyrighted instrument and may not be used or reproduced in whole or in part, in any form or language, or by any means without written permission of Psychological Assessment Resources.

REFERENCES

1. Ward RJ, Zucca FA, Duyn JH, Crichton RR, Zecca L. The role of iron in brain ageing and neurodegenerative disorders. *Lancet Neurol* 2014;13:1045-1060
2. Aquino D, Bizzi A, Grisoli M, Garavaglia B, Bruzzone MG, Nardocci N, et al. Age-related iron deposition in the basal ganglia: quantitative analysis in healthy subjects. *Radiology* 2009;252:165-172
3. Buijs M, Doan NT, van Rooden S, Versluis MJ, van Lew B, Milles J, et al. In vivo assessment of iron content of the cerebral cortex in healthy aging using 7-tesla T2*-weighted phase imaging. *Neurobiol Aging* 2017;53:20-26
4. Lane DJR, Ayton S, Bush AI. Iron and Alzheimer's disease: an update on emerging mechanisms. *J Alzheimers Dis* 2018;64(S1):S379-S395
5. McCarthy RC, Sosa JC, Gardeck AM, Baez AS, Lee CH, Wessling-Resnick M. Inflammation-induced iron transport and metabolism by brain microglia. *J Biol Chem* 2018;293:7853-7863
6. Ropele S, Wattjes MP, Langkammer C, Kilsdonk ID, Graaf WL, Frederiksen JL, et al. Multicenter R2* mapping in the healthy brain. *Magn Reson Med* 2014;71:1103-1107
7. Moon Y, Han SH, Moon WJ. Patterns of brain iron accumulation in vascular dementia and Alzheimer's dementia using quantitative susceptibility mapping imaging. *J Alzheimers Dis* 2016;51:737-745
8. Cogswell PM, Wiste HJ, Senjem ML, Gunter JL, Weigand SD, Schwarz CG, et al. Associations of quantitative susceptibility mapping with Alzheimer's disease clinical and imaging markers. *Neuroimage* 2021;224:117433
9. Yim Y, Choi JD, Cho JH, Moon Y, Han SH, Moon WJ. Magnetic susceptibility in the deep gray matter may be modulated by apolipoprotein E4 and age with regional predilections: a quantitative susceptibility mapping study. *Neuroradiology* 2022;64:1331-1342
10. van Duijn S, Bulk M, van Duinen SG, Nabuurs RJA, van Buchem MA, van der Weerd L, et al. Cortical iron reflects severity of Alzheimer's disease. *J Alzheimers Dis* 2017;60:1533-1545
11. Spotorno N, Acosta-Cabronero J, Stomrud E, Lampinen B, Strandberg OT, van Westen D, et al. Relationship between cortical iron and tau aggregation in Alzheimer's disease. *Brain* 2020;143:1341-1349
12. Damulina A, Pirpamer L, Soellradl M, Sackl M, Tinauer C, Hofer E, et al. Cross-sectional and longitudinal assessment of brain iron level in Alzheimer disease using 3-T MRI. *Radiology* 2020;296:619-626
13. Ayton S, Fazlollahi A, Bourgeat P, Raniga P, Ng A, Lim YY, et al. Cerebral quantitative susceptibility mapping predicts amyloid-β-related cognitive decline. *Brain* 2017;140:2112-2119
14. Ayton S, Wang Y, Diouf I, Schneider JA, Brockman J, Morris MC, et al. Brain iron is associated with accelerated cognitive decline in people with Alzheimer pathology. *Mol Psychiatry* 2020;25:2932-2941
15. Yoon J, Gong E, Chatnuntawech I, Bilgic B, Lee J, Jung W, et al. Quantitative susceptibility mapping using deep neural network: QSMnet. *Neuroimage* 2018;179:199-206
16. Jung W, Yoon J, Ji S, Choi JY, Kim JM, Nam Y, et al. Exploring linearity of deep neural network trained QSM: QSMnet. *Neuroimage* 2020;211:116619
17. Yang J, Lee S, Moon Y, Lee J, Moon WJ. Relationship between cortical iron and diabetes mellitus in older adults with cognitive complaints: a quantitative susceptibility map study. *Investig Magn Reson Imaging* 2023;27:84-92
18. Petersen RC, Smith GE, Waring SC, Ivnik RJ, Tangalos EG, Kokmen E. Mild cognitive impairment: clinical characterization and outcome. *Arch Neurol* 1999;56:303-308
19. McKhann GM, Knopman DS, Chertkow H, Hyman BT, Jack CR Jr, Kawas CH, et al. The diagnosis of dementia due to Alzheimer's disease: recommendations from the National Institute on Aging-Alzheimer's Association workgroups on diagnostic guidelines for Alzheimer's disease. *Alzheimers Dement* 2011;7:263-269
20. Albert MS, DeKosky ST, Dickson D, Dubois B, Feldman HH, Fox NC, et al. The diagnosis of mild cognitive impairment due to Alzheimer's disease: recommendations from the National Institute on Aging-Alzheimer's Association workgroups on diagnostic guidelines for Alzheimer's disease. *Alzheimers Dement* 2011;7:270-279

https://doi.org/10.3348/kjr.2023.0490

21. Moon Y, Lim C, Kim Y, Moon WJ. Sex-related differences in regional blood-brain barrier integrity in non-demented elderly subjects. *Int J Mol Sci* 2021;22:2860
22. Park M, Moon WJ, Moon Y, Choi JW, Han SH, Wang Y. Region-specific susceptibility change in cognitively impaired patients with diabetes mellitus. *PLoS One* 2018;13:e0205797
23. Wardlaw JM, Smith EE, Biessels GJ, Cordonnier C, Fazekas F, Frayne R, et al. Neuroimaging standards for research into small vessel disease and its contribution to ageing and neurodegeneration. *Lancet Neurol* 2013;12:822-838
24. Klein A, Tourville J. 101 labeled brain images and a consistent human cortical labeling protocol. *Front Neurosci* 2012;6:171
25. Nordenskjöld R, Malmberg F, Larsson EM, Simmons A, Ahlström H, Johansson L, et al. Intracranial volume normalization methods: considerations when investigating gender differences in regional brain volume. *Psychiatry Res* 2015;231:227-235
26. Smith SM. Fast robust automated brain extraction. *Hum Brain Mapp* 2002;17:143-155
27. Li W, Wu B, Liu C. Quantitative susceptibility mapping of human brain reflects spatial variation in tissue composition. *Neuroimage* 2011;55:1645-1656
28. Wu B, Li W, Avram AV, Gho SM, Liu C. Fast and tissue-optimized mapping of magnetic susceptibility and T2* with multi-echo and multi-shot spirals. *Neuroimage* 2012;59:297-305
29. Kim HG, Park S, Rhee HY, Lee KM, Ryu CW, Rhee SJ, et al. Quantitative susceptibility mapping to evaluate the early stage of Alzheimer's disease. *Neuroimage Clin* 2017;16:429-438
30. van Rooden S, Versluis MJ, Liem MK, Milles J, Maier AB, Oleksik AM, et al. Cortical phase changes in Alzheimer's disease at 7T MRI: a novel imaging marker. *Alzheimers Dement* 2014;10:e19-e26
31. Thal DR, Rüb U, Orantes M, Braak H. Phases of A beta-deposition in the human brain and its relevance for the development of AD. *Neurology* 2002;58:1791-1800
32. Thal DR, Beach TG, Zanette M, Lilja J, Heurling K, Chakrabarty A, et al. Estimation of amyloid distribution by [18F]flutemetamol PET predicts the neuropathological phase of amyloid β-protein deposition. *Acta Neuropathol* 2018;136:557-567
33. Collij LE, Heeman F, Salvadó G, Ingala S, Altomare D, de Wilde A, et al. Multitracer model for staging cortical amyloid deposition using PET imaging. *Neurology* 2020;95:e1538-e1553
34. Braak H, Alafuzoff I, Arzberger T, Kretzschmar H, Del Tredici K. Staging of Alzheimer disease-associated neurofibrillary pathology using paraffin sections and immunocytochemistry. *Acta Neuropathol* 2006;112:389-404
35. Greicius MD, Srivastava G, Reiss AL, Menon V. Default-mode network activity distinguishes Alzheimer's disease from healthy aging: evidence from functional MRI. *Proc Natl Acad Sci U S A* 2004;101:4637-4642
36. He X, Qin W, Liu Y, Zhang X, Duan Y, Song J, et al. Abnormal salience network in normal aging and in amnestic mild cognitive impairment and Alzheimer's disease. *Hum Brain Mapp* 2014;35:3446-3464
37. Rosenberg PB, Nowrangi MA, Lyketsos CG. Neuropsychiatric symptoms in Alzheimer's disease: what might be associated brain circuits? *Mol Aspects Med* 2015;43-44:25-37
38. Moon Y, Moon WJ, Kim H, Han SH. Regional atrophy of the insular cortex is associated with neuropsychiatric symptoms in Alzheimer's disease patients. *Eur Neurol* 2014;71:223-229
39. You SC, Walsh CM, Chiodo LA, Ketelle R, Miller BL, Kramer JH. Neuropsychiatric symptoms predict functional status in Alzheimer's disease. *J Alzheimers Dis* 2015;48:863-869
40. Sun W, Ueno D, Narumoto J. Brain neural underpinnings of interoception and decision-making in Alzheimer's disease: a narrative review. *Front Neurosci* 2022;16:946136
41. Kumar A, Fontana IC, Nordberg A. Reactive astrogliosis: a friend or foe in the pathogenesis of Alzheimer's disease. *J Neurochem* 2023;164:309-324
42. Marutle A, Gillberg PG, Bergfors A, Yu W, Ni R, Nennesmo I, et al. (3)H-deprenyl and (3)H-PIB autoradiography show different laminar distributions of astroglia and fibrillar β-amyloid in Alzheimer brain. *J Neuroinflammation* 2013;10:90
43. van Bergen JMG, Li X, Quevenco FC, Gietl AF, Treyer V, Meyer R, et al. Simultaneous quantitative susceptibility mapping and flutemetamol-PET suggests local correlation of iron and β-amyloid as an indicator of cognitive performance at high age. *Neuroimage* 2018;174:308-316
44. Bulk M, van der Weerd L, Breimer W, Lebedev N, Webb A, Goeman JJ, et al. Quantitative comparison of different iron forms in the temporal cortex of Alzheimer patients and control subjects. *Sci Rep* 2018;8:6898
45. Gong NJ, Dibb R, Bulk M, van der Weerd L, Liu C. Imaging beta amyloid aggregation and iron accumulation in Alzheimer's disease using quantitative susceptibility mapping MRI. *Neuroimage* 2019;191:176-185
46. McIntosh A, Mela V, Harty C, Minogue AM, Costello DA, Kerskens C, et al. Iron accumulation in microglia triggers a cascade of events that leads to altered metabolism and compromised function in APP/PS1 mice. *Brain Pathol* 2019;29:606-621
47. Joseph-Mathurin N, Dorieux O, Trouche SG, Boutajangout A, Kraska A, Fontès P, et al. Amyloid beta immunization worsens iron deposits in the choroid plexus and cerebral microbleeds. *Neurobiol Aging* 2013;34:2613-2622